# Comparison of Damage Probabilities of Buildings based on Ground Motion Prediction Models and Recorded Ground Motions for Christchurch Earthquakes

**S.R. Uma**
*GNS Science, P O Box 30368, Lower Hutt, New Zealand*

**SUMMARY:**

Christchurch City experienced a direct hit from a destructive Mw 6.2 aftershock earthquake following the main event of Mw 7.1 on the 4th September, 2010. The main event generated a response spectrum approximately close to design spectrum for Christchurch city. However, ground motions from the February event far exceeded the NZS 1170.5:2004 design spectrum with 500 year return period for which normal structures are designed for. This paper provides a review of ground motion characteristics of the September and February events and compares ground recorded spectra with various ground motion prediction models. The vulnerability of building stock in the Central Christchurch is assessed through a probabilistic displacement-based approach. The numerical study shows that the damage estimates are high for the February event compared to the code-based demands and demands predicted by various attenuation models. The paper demonstrates the importance of accounting for significant sources of uncertainties and variability while performing regional loss assessment.

*Keywords: Displacement-based approach, Ground motion prediction models, Building vulnerability assessment*

## 1. INTRODUCTION

The tectonic setting of New Zealand is marked by the boundary of the Australian and Pacific plates as shown in Figure 1, and the whole country is consequently seismically active. The seismic hazard model for New Zealand comprises many known active faults and background seismicity. On 4th September, 2010, Christchurch, the second largest city of New Zealand, was shaken by a Mw 7.1 earthquake, from the rupture of unknown faults. The epicentre was located near Darfield, about 40 km west of the main city. Two significant aftershocks with magnitude exceeding Mw 6.0 occurred on 22nd February 2011 (Mw 6.2) and 13th June 2011 (Mw 6.0). The locations of epicentres and the sequence of aftershocks (as of 13th March, 2012) are shown in Figure 2. The surface fault rupture was located near Greendale (20 km west to Christchurch) for the September event and the other two major aftershocks featured only sub-surface fault ruptures. The epicentre for 22nd February 2011event was about 10 km distance to the south-east of the central city and for the 13th June event the epicentre was further to the east. The impact of the last event was 'small' compared to other two events.

The September event inflicted minor to moderate levels of structural damage depending on the location, shaking intensity and building typology. A few cases of partial collapse of unreinforced masonry buildings were observed. Damage to non-structural components and contents was widespread in many buildings. Disruption to business in many commercial buildings was mainly attributed to non-structural damage. The impact of the February event in Christchurch on the built-environment was huge and destructive. Depending on the location and typology of the building, the extent of damage varied. The impact was more clearly pronounced within the central business district (CBD), where a variety of building typologies was subjected to severe ground shaking intensity and liquefaction. Special bulletin reports on preliminary observations and understanding of ground motion characteristics, structural and geotechnical aspects from the September and February events were published by the NZSEE[2010 and 2011]. Some parts of the CBD are still treated with restricted access due to on-going detailed assessment of damaged buildings and demolition process.
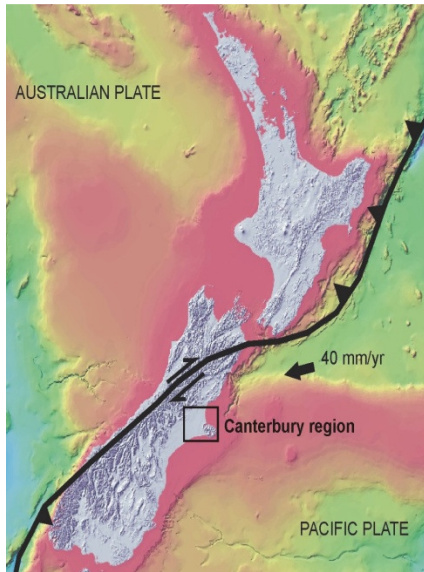
Figure 1. Tectonic setting of New Zealand(Courtesy: Kate Clark, GNS)
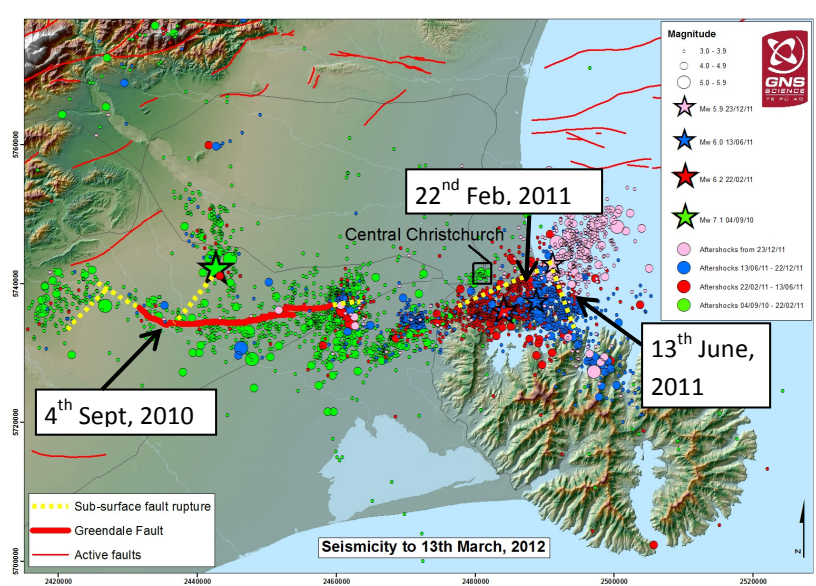
Figure 2. Details of main-shock and aftershocks since 4th Sept 2010 in Christchurch region (Courtesy: GeoNet, Rob Langridge, GNS).

The knowledge of regional damage distribution following a natural disaster is vital to support planning and decision making for emergency purposes. A multi-hazard loss modelling tool for New Zealand, "Riskscape" features different modules to handle various types of natural hazards [King and Bell, 2009]. As an integrated component of the tool for vulnerability assessment of buildings, a displacement-based approach within a probabilistic framework has been developed [Uma and Bradley, 2010a]. Ground motion prediction models can also be directly used to estimate the ground motion intensities, given the source-site related parameters.

In this paper, a brief summary on the intensity of ground motions recorded at seismic stations closer to CBD region is given with respect to the September and February events. The spectra are compared with those from ground motion prediction models. Displacement-based methodology is used to determine probabilistic estimates of damage distribution of typical building classes under spectral demands from the February event and compared with spectral demands specified in NZS 1170.5:2004 for 500 year return period event for normal structures (referred as design-based earthquake in this paper). The effects of variability in ground motion intensity models are highlighted.

## 2. GROUND MOTIONS

The GeoNet monitoring network in New Zealand, operated within GNS Science, contributes to the collection and utilisation of strong ground motion data. These include both national scale and regional scale strong motion networks, and a building response monitoring programme [Cousins and McVerry, 2009; Uma *et al*., 2011a]. The strong motion network provided rich sets of ground motion records within Christchurch region. Processed records are available at ftp.geonet.org.nz/strong/processed/Proc. Figure 3 shows plots of maximum horizontal and vertical accelerations recorded in both the September and February earthquakes in and around Christchurch. Close to the CBD there are four strong motion stations (i.e. CBGS – Christchurch Botanical Gardens, REHS – Christchurch Resthaven, CHHC-Christchurch Hospital, and CCCC – Christchurch Cathedral College). It is clear that the ground motions within the central city and to the east of the city were much stronger in the February event than in the September event. General note is that the ground accelerations were much higher than the expected given the magnitude and the distance of the earthquake. The ground motions recorded in central Christchurch generally considerably exceeded the 500-year or 1000-year spectra for which most of the buildings are designed. The February event was also characterised by very high vertical acceleration.
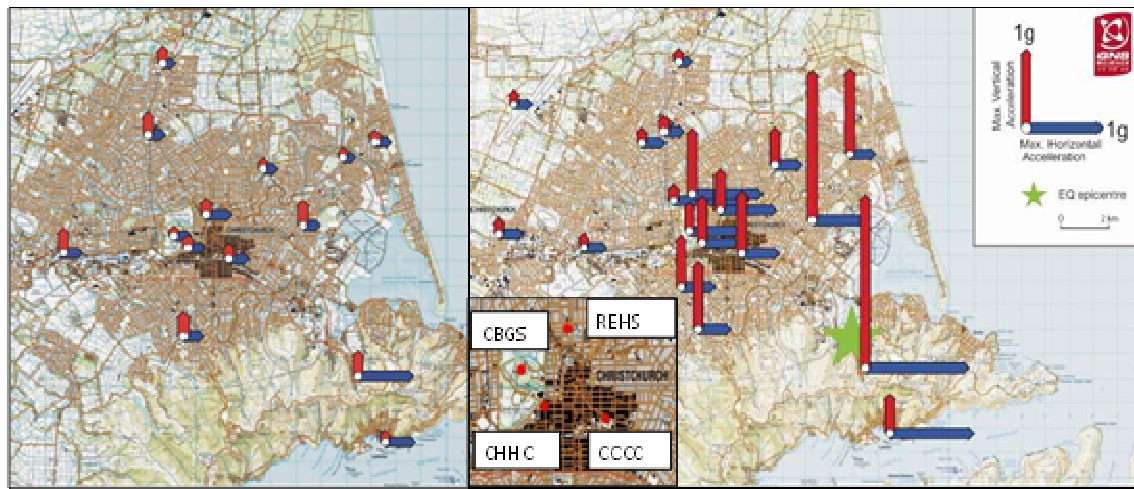
(a) Sept 4th 2010 event          (b) February 22nd 2011 event

Figure 3. Peak ground acceleration plot at strong motion stations; the inset (shaded region) shows Central Business District (CBD) area and strong motion sensor stations. (Courtesy: Anna Kaiser, & Jim Cousins, GNS)

## 2.1 Response at CCCC station

Figure 4 shows the acceleration record from CCCC station located within CBD from the September event and the February event. The records show evidence of liquefaction as observed in the field. The September event generated smaller peak ground acceleration of longer duration than the February event which exhibited stronger motion with shorter duration. It is interesting to note that in the September event, the shaking was predominantly aligned in the North-South (N-S) direction and in the February event it was more uniform, being stronger in the East-West (E-W) direction than experienced in the September event as shown in Figure 5.
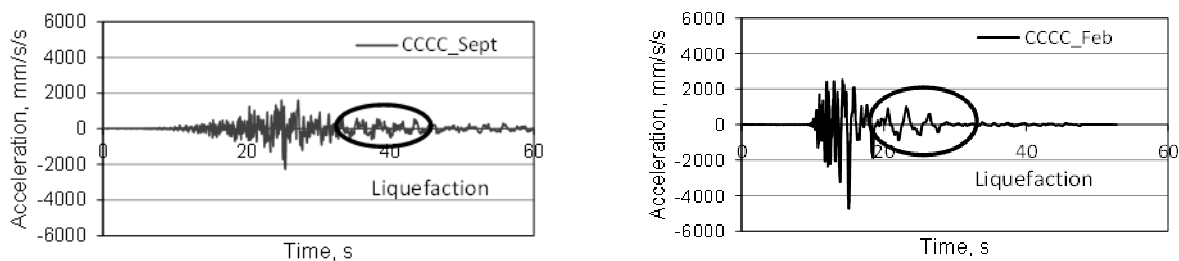


Figure 4. Acceleration records from CCCC station from the September (N-S) and February (E-W) components

Interestingly, most of the streets in the CBD are aligned in (N-S) and (E-W) directions which mean that the principal directions of the majority of the buildings are aligned N-S and E-W. However, the strong motion sensors are oriented arbitrarily (e.g. at CCCC the orientations are N26W and N64E). Response spectra for recorded components and projected to N-S, E-W directions are plotted in Figure 6. Publications in Seismological Research Letters (2011) explains that in the September event, site and basin effects contributed for the peak in long period range (2 and 3 seconds) and in the February event, the source (directivity) effects, site and basin effects could have contributed to peaks (between 1 and 2 seconds and about 3 seconds). In this station, the geometric mean of recorded components slightly exceeds the geometric mean of projected components, particularly near the peak regions. Note that the projected components aligning in the principal direction of buildings are maximums in N-S direction in the September and in E-W direction in the February and they are much larger than the recorded geometric means. This observation indicates that structural engineers would find it relevant to deal with the larger components of the recorded motions, and at times sensor orientation can play a significant role in determining design seismic forces. Very high vertical accelerations from February event have alerted them to the need to consider its influence in designs/assessments.
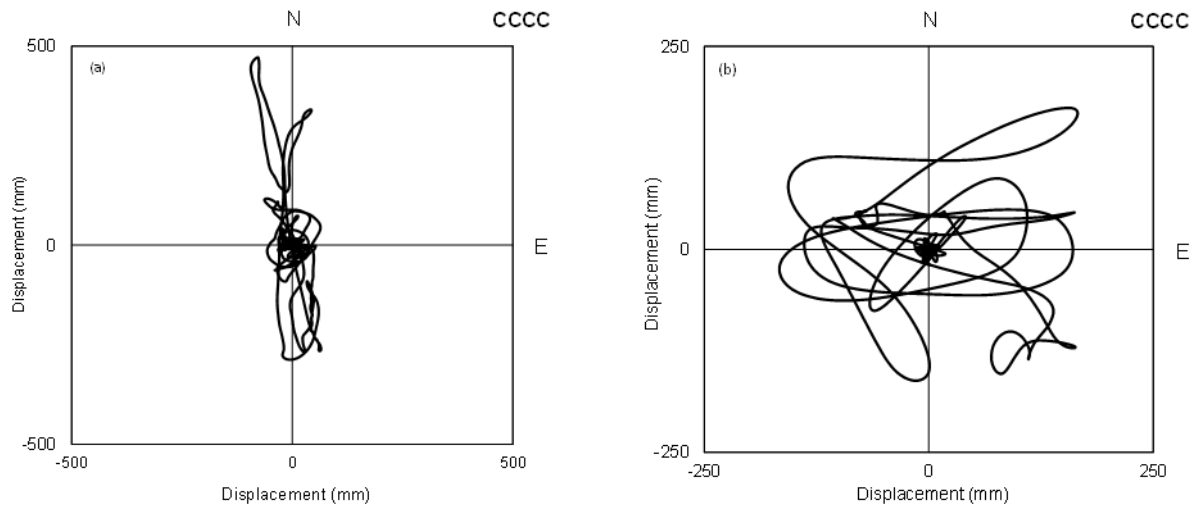
Figure 5. Ground displacement polar plots: (i) September; (ii) February events (Courtesy: Jim Cousins, GNS)
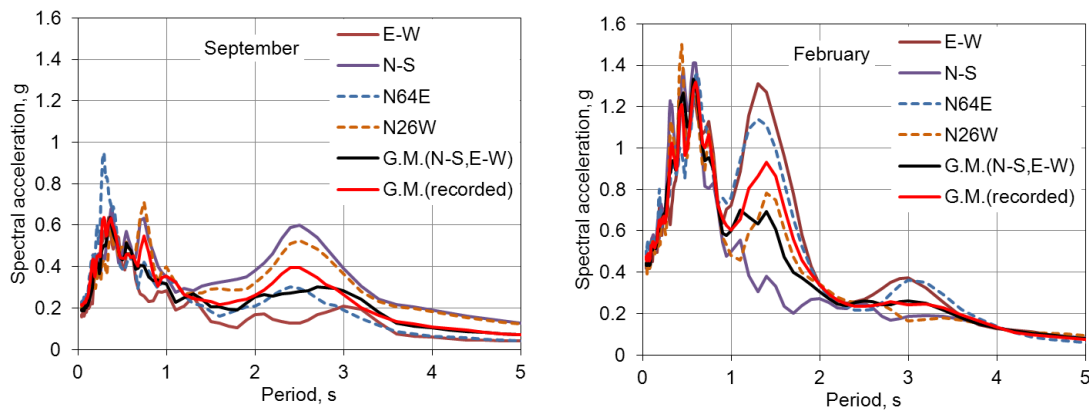


Figure 6. Response spectra from September and February events recorded at CCCC seismic station

## 2.2 Comparison of response spectra with predictions from attenuation models

Attenuation models use ground motion prediction equations (GMPE), and they provide estimates of ground motion intensity parameters in terms of geometric means (G.M) and standard deviations at different periods for a given earthquake scenario. Five different models are used to estimate spectral acceleration at the site represented by the CCCC station for the September and February events. The parametric values used in the attenuation models are listed in Table 2.1. (Personal communication with: Bill Fry and Caroline Holden, GNS Science).

**Table2.1.** Source-site parameters for CCCC station and earthquakes in September and February

| Parameters | September event | February event |
|---|---|---|
| Magnitude (Mw) | 7.1 | 6.2 |
| Fault-type | Strike-Slip | Oblique - Reverse |
| Rupture top depth (km) | 0 | 2 |
| Dip (degrees) | 89 | 65 |
| Vs 30 (m/s) – (estimated) | 200 | 200 |
| Depth 1.0 km/sec (m) | 700 | 700 |
| Distance to rupture (km) | 22.4 | 2.8 |
| (DistRup-DistJB)/DistRup | 0 | 0.0643 |
| (DistRup-DistX)/DistRup | -0.7170 | -0.6536 |
| Focal Depth (km) | 4 | 6 |
| Down-Dip width (km) | 5 | 10 |
| Rake angle (degrees) | 180 | 130 |

A few attenuation models (available in Open SHA) were used to generate spectral acceleration plots (represented by geometric means) and compared with recorded response spectra as shown in Figure 7. It appears that for the September event, all attenuation models considered in this study compare well with the recorded spectra except between 2 and 3 seconds characterised by amplification for the reasons mentioned earlier. However, for the February event, Chiou & Youngs (2008) and Bradley (2010) models matched the response spectra better than the other three models (McVerry *et al*., (2006), Boore and Atkinson (2008) and Abrahamson & Silva (2008)). Note that the high amplification peaks were not identified by any of the five attenuation models. This is due to the inherent inability of attenuation models to account for specific details related to site and source effects. It is worth noting that E-W components from September and February events have shown a peak at 3 seconds consistently and only recorded significant amplification between 1 and 2 seconds during February event. This could be due to added directivity effect combined with other site and basin effects.
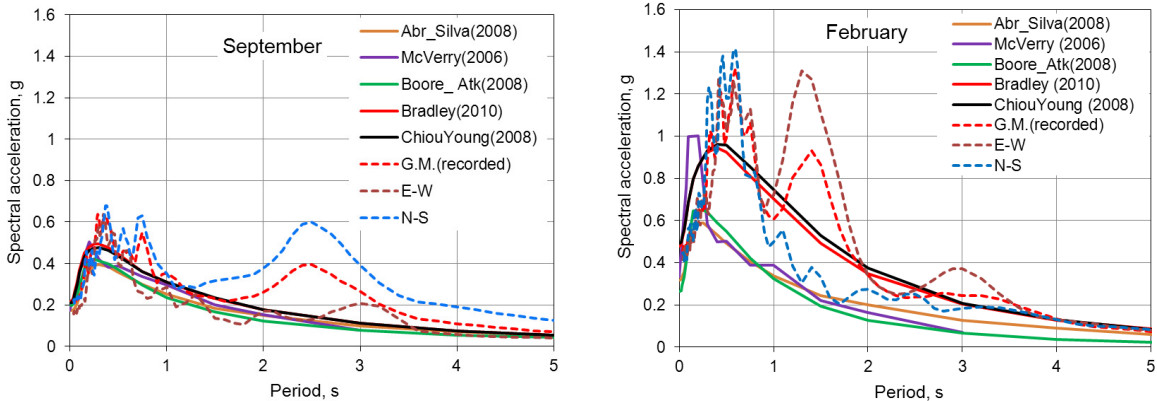


Figure 7. Comparison of response spectra plots from attenuation models and recorded at CCCC station

## 4. ACCELERATION-DISPLACEMENT RESPONSE SPECTRA

The acceleration-displacement-response-spectra (ADRS) plot is a convenient way to represent the capacity and demand spectra together along with period as radiating lines. Spectral demands in E-W direction of ground motions recorded in all the four CBD stations and NZS design spectrum are shown in Figure. 8 in ADRS format to appreciate the impact on buildings with different periods.
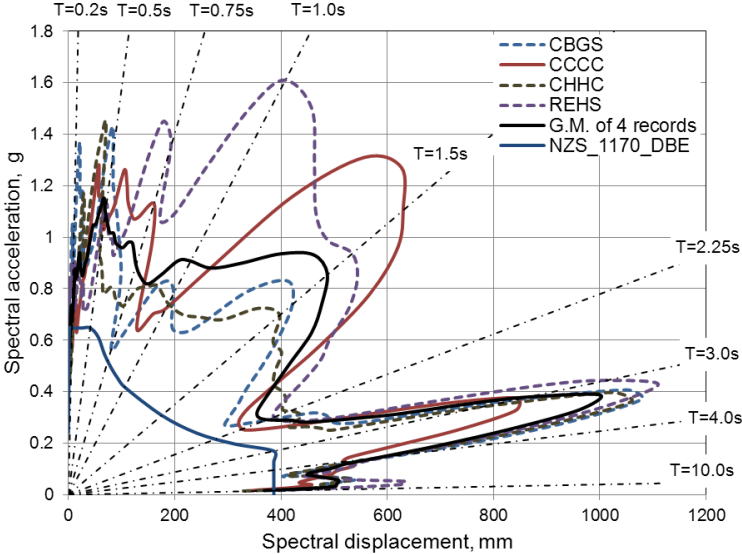


Figure 8. ADRS plot for E-W components for 4 stations (CBD) in February event

It is clear from the ADRS plot of spectral quantities that all the four records exceeded the DBE design spectrum. Considering the individual records, REHS and CCCC stations recorded much stronger accelerations than CHHC and CBGS stations. Referring to Figure 8, it can be stated that low-rise buildings with period range of 0.2s to 0.5s, experienced high demands. On the other hand, buildings with period larger than 0.5 s and up to 2 s (i.e. mid-rise and high-rise buildings), might have experienced very high demands compared to their capacity. Large displacement demands as high as 1m could have been experienced by high-rise flexible buildings with period closer to 3s. Only a few buildings in this period range existed in Christchurch at the time of the event. However, at about 2.25s, the demands sharply reduced and are closer to DBE.

## 5. OBSERVED PERFORMANCE OF BUILDINGS IN CBD

Old houses and commercial buildings with shops/office spaces constructed in the early 20th century, or in some cases in the 19th century had single or double brick walls for their structural integrity. Partial/full collapse of walls and roof components of such buildings involved failure of connecting elements. Given the intensity of the February event, many multi-storey buildings did well in terms of 'life-safety' and 'collapse prevention' performance objectives with the exception of two older reinforced concrete buildings. The overall performance was 'as expected' and could be attributed to the short duration of the earthquake. In multi-storey buildings, various components including main lateral load resisting elements, gravity load elements, floor diaphragms, reinforced concrete shear walls were tested for their individual capacities and also their role towards integral performance of the whole structure. High vertical accelerations could have imparted heavy axial loads in columns wherein the effect of confinement reinforcement becomes significant to prevent/control exploding failure of columns. In pre-1970 buildings, multiple shear failures in beam column joints and short column failures were observed. Damage to beams with insufficient splice in reinforcement bars was noted. Older frames with infill suffered shear failure in beams and infill walls.

Lightly reinforced structural walls suffered buckling failure of reinforcement. In multi-storey buildings, structural elements designed only for gravity loads suffered severe damage lacking the ability to deform along with other ductile elements. In 1976-era reinforced concrete medium-rise to high-rise buildings, bars in boundary columns of shear walls showed buckling failure. In some cases, confinement steel ties fractured in boundary columns. In post 1990 buildings slender reinforced concrete walls suffered buckling of reinforcement, probably due to high vertical acceleration-induced axial loads. Precast-floors in reinforced concrete frames suffered lack of seating from supporting beams due to beam elongation resulting from plastic hinges in beams [NZSEE, 2011].

Reinforced concrete moment resisting frame buildings with lift-shafts constructed with light timber partitions rather than with concrete shear walls cores led to the damage of stairs and lift-guides due to relatively large inter-storey drifts. On the other hand, lift cores with concrete-shear walls provided lateral stiffness to the building, controlling inter-storey drifts between floors and reduced damage. In two high-rise buildings, precast staircases collapsed. One of the reasons could be attributed to the unseating of the staircase elements due to excessive drift demands. Also, staircases being stiff elements connecting two consecutive floor levels, could potentially introduce torsional demands in the building when out-of-phase displacement at floor levels occurs during dynamic response.

Needless to say, non-structural elements (ceilings, interior partition walls, facades and building services) suffered extensive damage. In some buildings, even if structural damage was minimal, damage to ceilings and other utilities restricted access to buildings and disrupted business continuity. Falling of ceiling panels and facades could potentially lead to life-safety risks. Apart from buildings, many tall and heavily loaded pallet racks collapsed in industrial storage facilities located near the epicentre area [Uma and Beattie, 2011b].

Foundation settlement and tilting occurred in buildings (both with shallow and deep foundations) located close to rivers due to liquefaction. There were cases of ground settlement or foundation failures.

# 6. DISPLACEMENT BASED APPROACH TO ESTIMATE DAMAGE PROBABILITIES

In this section, a probabilistic displacement-based framework to determine the probabilities of failure or being in various damage-limit states for different building classes [Uma and Bradley, 2010a] is discussed. For illustrative purposes, a building class (medium rise ductile reinforced concrete (RC) frame building) is assumed to be subjected to CCCC records and its likely damage probabilities under February earthquake scenario are analysed. Spectral demands are obtained from: (i) actual recorded data by the seismic sensor and (ii) an attenuation model (e.g. Bradley 2010). As per the capacity spectrum concept, the capacity curve of the building and spectral demands from ground motions are plotted in Figure 9 showing the plots of: (i) pushover capacity curve of the building; (ii) E-W component; (iii) geometric mean (G.M.) of components (N26W and N64E); (iv) geometric mean of (E-W, N-S) components; (v) 500-year return period 'design spectrum' as per NZS 1170.5:2004 (neglecting short-term enhancement of seismicity in Christchurch region); (vi) prediction by Bradley (2010) model; and (vii) 84th percentile prediction by Bradley (2010) model. It can be appreciated that 'variability' is the prominent feature within spectral demands computed from various sources as listed above. Note that the 'design spectrum' is based on probabilistic seismic hazard analyses and represents the larger component whereas all other spectra are scenario based. Variation is particularly pronounced near the peak amplifications.

It is imperative that the regional assessment tools should carefully adopt building models representing the 'true' characteristics of the building stock of interest and do not rely on the models developed for any other region or country [Uma *et al*., 2011c]. The probabilities of failure or damage can be estimated by comparing spectral demands with building capacity. Even though capacity curve can have associated variability, it is expected to be significantly small compared to the variability associated with ground motion spectral demands. Looking at Figure 9, it is very self-explanatory that the choice of spectral demand would greatly influence the estimation of damage probabilities.

The methodology considers a typical building representing a building class as an equivalent single degree of freedom (SDOF) oscillator. The steps involved are: (i) simulation of building characteristics through Monte-Carlo procedure; (ii) determination of building displacement (or drift ratio at equivalent height of SDOF) at various damage limit states; (iii) determination of effective period corresponding to the damage limit states (LS); (iv) Obtaining spectral displacement demand at the effective period; and (v) estimation of damage state probability by comparing the displacement realised by the building and the earthquake demand considering various sources of uncertainties related to building and ground motion parameters. The building characteristics are listed in Table 6.1.
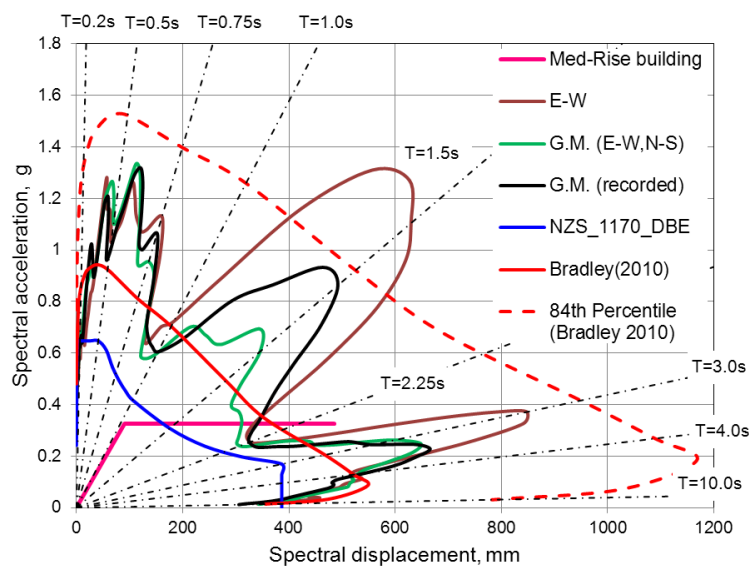


Figure 9. Idealised bilinear capacity curve for medium-rise building with spectral demand curves

## 6.1 Definition of Damage Limit States

The damage states are generally related to the structural response parameter such as average roof drift ratio considered as its maximum response. The relationship between the damage state and the displacement is difficult to establish. It requires a large amount of information on damage sustained by all structural elements for a given building type and sound engineering judgement. Also, some studies have recommended considering residual displacements in combination with maximum transient displacements in defining performance objectives for buildings [Uma *et al*., 2010b]. In this study, four limit states are defined in terms of only maximum roof drift ratio (LS1 to LS4). LS1 denotes the 'significant yield point' which is the bifurcating point in a bilinear, elastic-plastic, baseshear-roof drift curve. LS3 is considered at a drift limit corresponding to ultimate limit state satisfying the life-safety criteria at design based earthquake with a 500 year return period. LS4 is considered to be at the drift limit corresponding to collapse prevention criteria. LS2 is defined mid-way between LS1 and LS3. It is implicit that LS0 indicates a scenario of 'no-damage' in the building. The proposed methodology assumes that the building meets the damage limit states in a progressive manner, i.e. LS2 can happen only after LS1 has occurred and so on. The drift ratios chosen in this study are based on recommendations from FEMA 273(1997) and NZS1170.5:2004. Median ($median\_D_{LSi}$) and dispersion($\beta\_D_{LSi}$) of damage limits can be expressed in terms of respective median and dispersion of yield displacement and ductility (μ) experienced at that limit state.

**Table 6.1.** Initial and damage limit state parameters considered for a typical medium-rise RC frame

| Initial Parameters | | | | | | | |
|---|---|---|---|---|---|---|---|
| Median | Dispersion | Median | Dispersion | Median | Dispersion | Median | Dispersion |
| Initial Period, $T_y$ | | Yield displacement, $D_y$ | | Effective height | | | |
| 1.1s | 0.24 | 0.09m | 0.35 | 12m | 0.15 | | |
| Damage Limit States | | | | | | | |
| LS1 | | LS2 | | LS3 | | LS4 | |
| 0.09m | 0.35 | 0.18m | 0.4 | 0.3m | 0.46 | 0.48m | 0.53 |

## 6.2 Effective period of building at damage limit state

The methodology adopts a simple equation to calculate the effective period which is related to initial period and ductility that is achieved at the chosen damage limit state [Priestley *et al*., 2007].

## 6.3 Seismic displacement demand from earthquake scenario at damage limit states

For a given damage limit state, the site period is assumed to be equal to the building effective period to simulate the maximum impact. Note that in the simplified formulation used it is assumed that the uncertainty in the capacity and demand arising from the uncertainty in initial period, Ty, are uncorrelated. While this is strictly not correct it allows an uncoupling of the capacity and demand relationships, which is desirable from both a practical and computational point of view, and is consistent with other simplifying assumptions made in the methodology. The elastic spectral displacement demands are reduced using spectra reduction factor, ψ_eff as in Eqn. 6.1 to represent inelastic spectral displacement demands at various damage limit states, where equivalent viscous damping ratio ξ_eff as in Eqn. 6.2 is obtained using the ductility level achieved at a given damage limit state and the damping reduction factor, η for a given structural system as suggested by Priestly *et al*., 2007. For example, the damping reduction factor for reinforced concrete frame building is 0.565.

$$\psi_{eff} = \sqrt{0.07/\left(0.02 + \xi_{eff}\right)}$$
(6.1)

$$\xi_{eff} = 0.05 + \eta\left((\mu - 1)/\mu\right)$$
(6.2)

The median spectral displacement demand $median\_S_{d(demand)}$ at effective periods can be obtained from Figure 9 after accounting for respective reduction factors. In this study, the dispersion of spectral displacement $\beta\_S_{d(demand)}$ is taken as 0.5 at all periods even though it varies with respect to period.

## 6.2 Probability of building damage state

The probability of building damage state is determined by comparing the spectral displacement demand with spectral displacement of the structure considering the uncertainty into account. The cumulative probability of any damage state is expressed as given in Eqns. 6.3. In this methodology, the demand and capacity are independent because the dependence between Ty is neglected.

$$Z = \left| \frac{\ln\left(median\_S_{d(demand)} / median\_D_{LSi}\right)}{\sqrt{\left(\beta\_D_{LSi}\right)^2 + \left(\beta\_S_d\left(demand\right)\right)^2}} \right| \tag{6.3}$$

Using standard normal cumulative distribution function, the cumulative probability of a given damage state can be computed as in Eqn. 6.4:

$$P_f = \Phi(Z) \tag{6.4}$$

As mentioned earlier, the limit states are assumed to occur in progressive manner. Based on this assumption, the cumulative probability of failure corresponding to a damage states can be expressed as combined probabilities. For example, the probability of failure at LS2 is $P_f(LS1)*P_f(LS2)$ and so on.

Probability of being only in that damage state can be obtained as the difference between cumulative probabilities of consecutive damage limit states. Figures 10(a) and (b) show comparisons of damage probabilities of medium-rise RC ductile frames for all three demand scenarios.
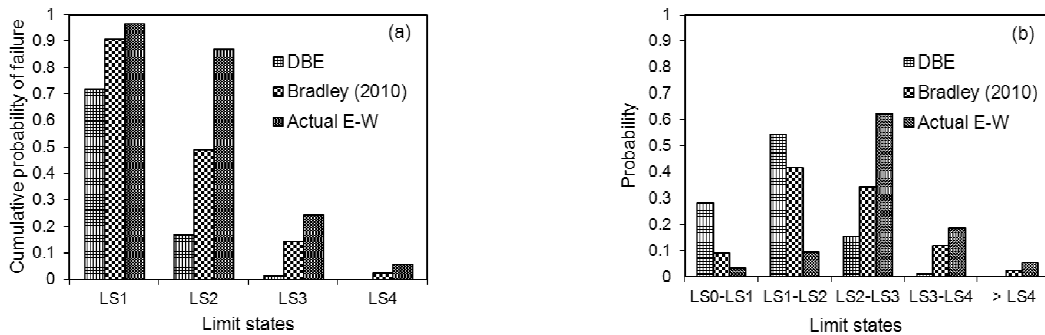


Figure 10. Damage probabilities for spectral demands based on DBE, attenuation model and 'Actual' scenarios

It is very clear that the distribution of damage probabilities varies significantly between the spectral demand models (theoretical and actual) adopted. For example, DBE model shows about 60% of the chosen building typology to be in lower damage states (i.e. between LS1-LS2) and almost none beyond LS4. However, under 'actual' earthquake demand 60% of buildings could have reached to 'life-safety' limit state and about 6% of building stock exceeding LS4. Hence, much attention needs to be given in understanding the earthquake hazard associated with the region in loss assessments. The computed damage distribution is believed to be representative of actual damage distribution. However, in reality the relationship between the damage level and the need for demolition seems to be influenced by other factors such as insurance industry, market value and business interruption.

## 8. SUMMARY

In this paper, the spectral characteristics of ground motions from the September and February events, recorded close to CBD of Christchurch, were compared to explain the intensity of ground motions and the damage caused. Also, ground motion intensities were predicted using five different attenuation models and the variation between models were demonstrated. The observed performance of buildings, particularly in CBD was summarised. A probabilistic displacement-based approach was adopted to assess the vulnerability of the building stock in Christchurch. The methodology gives a better appreciation of the proportion of damaged building stock and their degree of damage and therefore

may be very useful to assess regional loss. A typical medium-rise reinforced concrete ductile frame building was chosen to be assessed under the demands from the February event, the code-specified demands from Design-basis earthquake and a ground motion prediction attenuation model. Huge uncertainties involved in the ground motion predictions and actual ground motion characteristics could result in variation in estimated damage probabilities and observed damages in building stock.

## ACKNOWLEDGEMENTS

## REFERENCES

Abrahamson, N. A., and Silva, W.J. (2008), Summary of the Abrahamson & Silva NGA Ground-Motion Relations. *Earthquake Spectra*, **24:1**, pp. 67-97.

Bradley, B.A. (2010) NZ-specific pseudo-spectral acceleration ground motion prediction equations based on foreign models. Report No.2010-03, Department of Civil and Natural Resources Engineering, University of Canterbury: Christchurch, New Zealand. 324

Boore, D. M. and Atkinson, G.M. (2008). Ground-motion prediction equations for the average horizontal component of PGA, PGV, and 5%-damped PSA at spectral periods between 0.01 s and 10.0 s. *Earthquake Spectra,* **24:1**,pp. 99—138

Chiou, B. and Youngs, R. (2008). A NGA Model for the Average Horizontal Component of Peak Ground Motion and Response Spectra, *Earthquake Spectra*, **24:1**, pp.173-215.

Cousins, W.J. and McVerry, G.H. (2009). New Zealand Strong Motion Network Development Plan. 1999-2009. *GNS Science Report* 2009/44, August 2009. 41p. 5 Maps.

FEMA 273 (1997). Federal Emergency Management Agency. NEHRP Guidelines for Seismic Rehabilitation of Buildings. Federal Emergency Management Agency Report. Washington D.C.

King, A.B. and Bell, R.(2009). Riskscape Project. 2004-2008, *GNS Science Consultancy Report*. 2009/247, p162.

McVerry GH, Zhao JX, Abrahamson NA and Somerville PG. 2006 New Zealand acceleration response spectrum attenuation relations for crustal and subduction zone earthquakes. *Bulletin of the New Zealand Society for Earthquake Engineering*; 39:4, pp. 1-58

NZS1170.5. (2004).Structural Design Actions Part 5 Earthquake actions - New Zealand, Standards New Zealand, Wellington, New Zealand.

NZSEE. (2010). Preliminary Observations of the September 2010 Darfield (Canterbury) Earthquake Sequence. *Bulletin of the New Zealand Society of Earthquake Engineering*. **43:4**, (whole issue), December, 439p

NZSEE. (2011). Special Bulletin on February 2011 event in Christchurch. *Bulletin of the New Zealand Society of Earthquake Engineering*. **44:4**, (whole issue), December, 430p

OpenSHA: http://www.opensha.org/

Priestley, M.J.N., Calvi, G.M. and Kowalsky, M.J. (2007). Displacement-based seismic design of structures. IUSS Press, Pavia, Italy

Seismological Research Letters (2011). 22 February 2011 6.2 Magnitude Earthquake in Christchurch, New Zealand. **82:6**. http://www.seismosoc.org/news/newsitem.php?id=i20111110761

Uma, S.R. and Bradley, B.A. (2010a). Development of Displacement-Based New Zealand Building Fragility Functions for Ground Motion Hazard. *GNS Science Report*. 2010/33. 22p

Uma, S.R., Pampanin, S. and Christopoulos, C. (2010b). Development of Probabilistic Framework for Performance-Based Seismic Assessment of Structures Considering Residual Deformations. *Journal of Earthquake Engineering*, **14:7**, pp.1092-1111.

Uma,S.R., King, A.B., Cousins, W.J., and Gledhill, K. (2011a). The GeoNet Building Instrumentation Programme. *Bulletin of the New Zealand Society for Earthquake Engineering*. **44:1**, pp. 53-63.

Uma, S.R. and Beattie, G. (2011b). Observed Performance of Industrial Pallet Rack Storage Systems in Canterbury Earthquakes. *Bulletin of the New Zealand Society for Earthquake Engineering*. **44:4,** pp.388-393.

Uma, S.R., Ryu, H., Luco, N., Liel, A.B. and Raghunandan, M. (2011c). Comparison of Mainshock and Aftershock Fragility Curves Developed for New Zealand and US buildings. *9th Pacific Conference on Earthquake Engineering*, Auckland, Paper No. 227.